Topology in BEC

Tristan.W

December 30, 2025

Contents

1 * Solitons in the Gross–Pitaevskii Theory

1.1 Quasi-1D Gross–Pitaevskii equation and the healing length

We start from a quasi-one-dimensional (quasi-1D) Bose–Einstein condensate (BEC), where the transverse confinement is so strong that the transverse motion is frozen and the order parameter depends effectively only on the longitudinal coordinate x. Ignoring (for the moment) the longitudinal trapping potential $V(x)$, the time-dependent Gross–Pitaevskii (GP) equation reads

$$i\hbar\frac{\partial\psi(x,t)}{\partial t} = -\frac{\hbar^2}{2m}\frac{\partial^2\psi(x,t)}{\partial x^2} + U|\psi(x,t)|^2\psi(x,t), \tag{1}$$

where m is the atom mass and U is the effective 1D interaction strength.

In a uniform ground state, $\psi(x,t) = \sqrt{n_0}\,e^{-i\mu t/\hbar}$, where n_0 is the bulk density and the chemical potential is $\mu = Un_0$. A central length scale is the *healing length* ξ, defined by balancing kinetic and interaction energies:

$$\frac{\hbar^2}{2m\xi^2} = \mu = Un_0. \tag{2}$$

Physically, ξ sets the minimal distance over which the condensate amplitude can vary significantly without paying a large kinetic energy cost; it is also the characteristic size of "cores" where the density is depleted.

Why we discuss solitons first?

Solitons provide a technically clean entry point: Eq. (1) admits exact, explicitly verifiable nonlinear wave solutions. This allows one to establish (i) how ξ emerges as a core size, (ii) how rapid phase variation produces large superflow velocity, and (iii) how to compute excitation energies from an energy functional—all of which will reappear, with added topology, in the vortex problem.

1.2 Static dark soliton as an exact solution

Consider the stationary ansatz

$$\psi(x,t) = e^{-i\mu t/\hbar}\,\psi(x), \qquad \psi(x) = \sqrt{n_0}\,\tanh\!\left(\frac{x}{\sqrt{2}\,\xi}\right), \tag{3}$$

where n_0 is the bulk density and ξ is the healing length. Substituting $\psi(x,t) = e^{-i\mu t/\hbar}\psi(x)$ into Eq. (1) gives the time-independent GP equation

$$-\frac{\hbar^2}{2m}\frac{d^2\psi(x)}{dx^2} + U|\psi(x)|^2\psi(x) = \mu\psi(x). \tag{4}$$

Let $y \equiv x/(\sqrt{2}\xi)$. Using

$$\frac{d}{dy}\tanh y = \operatorname{sech}^2 y, \qquad \frac{d^2}{dy^2}\tanh y = -2\operatorname{sech}^2 y\,\tanh y, \qquad \operatorname{sech}^2 y + \tanh^2 y = 1, \tag{5}$$

we compute

$$\frac{d^2\psi}{dx^2} = \sqrt{n_0}\,\frac{d^2}{dx^2}\tanh\!\left(\frac{x}{\sqrt{2}\xi}\right) = \sqrt{n_0}\,\frac{1}{2\xi^2}\frac{d^2}{dy^2}\tanh y = -\sqrt{n_0}\,\frac{1}{\xi^2}\operatorname{sech}^2 y\,\tanh y. \tag{6}$$

Therefore,

$$-\frac{\hbar^2}{2m}\frac{d^2\psi}{dx^2} = \frac{\hbar^2}{2m\xi^2}\sqrt{n_0}\,\mathrm{sech}^2 y\,\tanh y, \qquad U|\psi|^2\psi = Un_0\sqrt{n_0}\,\tanh^3 y. \tag{7}$$

Using Eq. (2), $\hbar^2/(2m\xi^2) = Un_0 = \mu$, and Eq. (5),

$$-\frac{\hbar^2}{2m}\frac{d^2\psi}{dx^2} + U|\psi|^2\psi = \mu\sqrt{n_0}\left(\mathrm{sech}^2 y\,\tanh y + \tanh^3 y\right) = \mu\sqrt{n_0}\,\tanh y = \mu\psi, \tag{8}$$

which proves that Eq. (3) is an exact solution of Eq. (1).

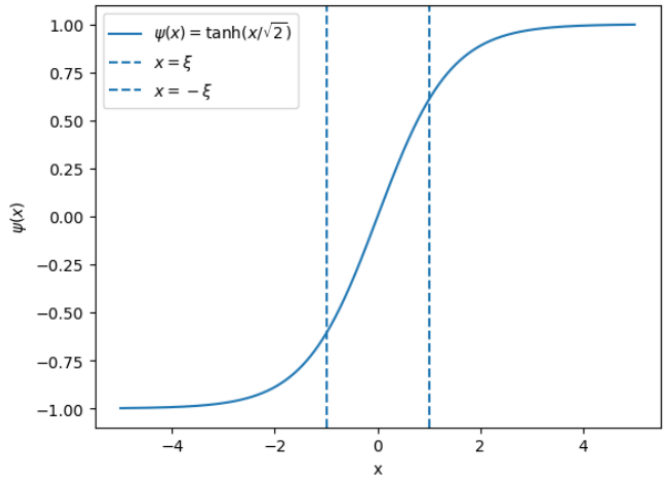

The static solution satisfies

$$\lim_{x\to+\infty}\psi(x) = +\sqrt{n_0}, \qquad \lim_{x\to-\infty}\psi(x) = -\sqrt{n_0}, \tag{9}$$

indicating a π phase difference between the two ends. The phase change is localized near the soliton center, where the density is strongly depleted over a length scale $\sim \xi$.

Physical interpretation: phase gradients, density depletion, and the meaning of ξ

A useful intuition comes directly from the GP energy functional written in amplitude–phase variables. Writing $\psi(\boldsymbol{r}) = \sqrt{n(\boldsymbol{r})}\,e^{i\theta(\boldsymbol{r})}$, one has

$$|\nabla\psi|^2 = \left|\nabla\sqrt{n}\right|^2 + n\,|\nabla\theta|^2. \tag{10}$$

In two dimensions (and in the absence of trapping potentials), the grand-canonical GP energy reads

$$\mathcal{E}[n,\theta] = \int d^2r\left[\frac{\hbar^2}{2m}\left(\left|\nabla\sqrt{n}\right|^2 + n|\nabla\theta|^2\right) + \frac{U}{2}n^2 - \mu n\right]. \tag{11}$$

The term $\frac{\hbar^2}{2m}n|\nabla\theta|^2$ shows that a rapid phase variation (large $|\nabla\theta|$, hence large superflow velocity $\boldsymbol{v} = (\hbar/m)\nabla\theta$) carries a kinetic-energy cost proportional to the *local density* n. For a fixed phase texture, lowering n in the region where $|\nabla\theta|$ is large reduces this kinetic-energy penalty. Thus, phase gradients naturally drive a *local depletion* of the condensate density: in energetic terms, the system prefers to "turn off" the order parameter amplitude where enforcing the phase pattern would otherwise be too costly.
Of course, depleting n is not free. The interaction and chemical-potential terms favor the bulk value $n_0 = \mu/U$, while the quantum-pressure term $\frac{\hbar^2}{2m}|\nabla\sqrt{n}|^2$ penalizes sharp spatial variations of the density. The healing length ξ is the scale set by this competition: it is the

characteristic distance over which the density can change appreciably while keeping the total energy minimal. Equivalently, ξ is the minimal length over which a locally suppressed density profile can "heal" back to its bulk value.

1.3 Moving solitons, Galilean invariance, and excitation energy

In the absence of external potentials, Eq. (1) is Galilean invariant. A moving dark soliton with velocity v can be written in the form

$$\psi(x,t) = \sqrt{n_0}\left[i\frac{v}{c} + \sqrt{1-\frac{v^2}{c^2}}\,\tanh\!\left(\frac{\sqrt{1-v^2/c^2}}{\sqrt{2}\,\xi}(x-vt)\right)\right]e^{-i\mu t/\hbar}, \tag{12}$$

where c is the sound velocity in the weakly interacting condensate. For a contact interaction, c is given by

$$c = \sqrt{\frac{\mu}{m}} = \sqrt{\frac{Un_0}{m}}. \tag{13}$$

It is convenient to define

$$s \equiv \sqrt{1-\frac{v^2}{c^2}}, \qquad \tilde{x} \equiv \frac{x-vt}{\sqrt{2}\,\xi}. \tag{14}$$

The moving solution Eq. (12) reduces to the static one Eq. (3) as $v \to 0$ and approaches the uniform ground state as $v \to c$. The bound $|v| \le c$ is consistent with the fact that solitons cannot move faster than sound in this mean-field setting.

Energy of a soliton.

A convenient way to define the excitation energy is to use the grand-canonical energy functional (in 1D)

$$\mathcal{E}[\psi] = \int dx\left[\frac{\hbar^2}{2m}\left|\frac{d\psi}{dx}\right|^2 + \frac{U}{2}|\psi|^4 - \mu|\psi|^2\right], \qquad \mu = Un_0. \tag{15}$$

For the uniform ground state $|\psi|^2 = n_0$, one finds $\mathcal{E}_g = -\frac{U}{2}n_0^2 L$ for a system of length L. Substituting Eq. (12) into Eq. (15) yields the exact excitation energy (relative to the uniform state),

$$\mathcal{E}_s - \mathcal{E}_g = \frac{8}{3\sqrt{2}}\frac{\hbar^2 n_0}{2m\xi}\left(1-\frac{v^2}{c^2}\right)^{3/2} = \frac{4\hbar m}{3U}\,(c^2-v^2)^{3/2}. \tag{16}$$

A notable feature is that the soliton excitation energy decreases as v increases and vanishes as $v \to c$, consistently with the disappearance of the density dip in that limit.

1.4 Solitons in a smooth trap and stability of the quasi-1D regime

Now include a smooth longitudinal confinement $V(x)$. In a local density approximation (LDA), the soliton energy is dominated by the core region of size $\sim \xi$, and one may replace c in Eq. (16) by the local sound speed at the soliton center X:

$$c(X)^2 = \frac{Un(X)}{m} \approx c_0^2 - \frac{V(X)}{m}, \tag{17}$$

where c_0 is the sound speed at the trap center. Assuming the soliton energy is conserved during motion and defining $v = dX/dt$, one arrives at an effective energy conservation law of the form

$$m\left(\frac{dX}{dt}\right)^2 + V(X) = \text{constant}, \tag{18}$$

which implies that, in a harmonic trap $V(X) = \frac{1}{2}m\omega^2 X^2$, the soliton oscillates with frequency $\omega/\sqrt{2}$. This can be interpreted as an effective particle of mass $2m$.

Finally, solitons are dynamically stable only in the quasi-1D regime where transverse excitations are suppressed. If the transverse size is much larger than ξ, transverse modes become relevant and a dark soliton may decay into vortex structures (e.g. vortex rings or vortex pairs), reflecting that in higher dimensions phase defects tend to reorganize into genuinely topological objects.

2 Vortices as Topological Defects in a Condensate

2.1 Why *Topology* kicks in?

At low energies, a single-component Bose–Einstein condensate is often introduced through its smooth hydrodynamic degrees of freedom: density and phase fluctuations of the order parameter $\psi = \sqrt{n}\, e^{i\theta}$. In this viewpoint, the gapless phonon is the Goldstone mode of the spontaneously broken global $U(1)$ symmetry, and a large fraction of long-wavelength physics can indeed be organized as an effective theory for a smooth phase field $\theta(\boldsymbol{r}, t)$. However, phonons do not exhaust the physically relevant excitations, because the Goldstone description implicitly assumes that θ is globally single-valued and smooth.

The missing ingredient is that the order parameter is not merely a local field but a map into an order-parameter manifold. For a condensate with nonzero density, the manifold of phases is $U(1) \simeq S^1$, and in two dimensions the boundary of a region is a loop S^1. As a result, field configurations can fall into distinct homotopy classes labeled by an integer winding number. A vortex is precisely a configuration in which θ winds by $2\pi\kappa$ around a core. Such a winding cannot be removed by any smooth deformation that keeps the order parameter well-defined everywhere; the system must allow a singular point where the amplitude collapses and the phase ceases to be defined. In this sense, vortices are *topological defects*: they are not additional small-amplitude normal modes, but nonperturbative configurations that reflect the global topology of the order parameter.

This distinction is not merely formal. Experimentally, vortices are routinely created and observed in ultracold gases: phase imprinting and stirring generate quantized circulation; interference measurements reveal dislocations associated with free vortices; and, in two dimensions, the proliferation of vortices under thermal fluctuations underlies the Berezinskii–Kosterlitz–Thouless mechanism and the universal jump of superfluid stiffness. None of these phenomena can be captured within a phonon-only description, because they involve configurations with nontrivial winding and cores where the condensate amplitude is strongly depleted.

Finally, it is worth emphasizing what is universal and what is model-dependent:

> The possibility of vortex defects is a general feature of $U(1)$ order parameters, as it follows from $\Pi_1(U(1)) = \mathbb{Z}$.

What depends on dimensionality and energetics is *how* vortices influence phases and dynamics: in 3D they form line defects whose excitations include Kelvin waves and reconnection processes, while in 2D their logarithmic energetics and entropy lead to the BKT scenario. Thus, discussing vortices is not an optional refinement but an essential complement to the Goldstone-mode (phonon) picture in a condensate.

2.2 Vortex Ansatz Wavefunction

We consider a quasi-two-dimensional condensate in the xy-plane. The essential input behind a vortex is *phase winding*: away from the defect, the condensate has a well-defined

phase $\theta(\boldsymbol{r})$ whose change along a closed loop can be nontrivial. Writing

$$\psi(\boldsymbol{r}) = \sqrt{n(\boldsymbol{r})}\, e^{i\theta(\boldsymbol{r})}, \tag{19}$$

the superfluid velocity field is

$$\boldsymbol{v}(\boldsymbol{r}) = \frac{\hbar}{m}\nabla\theta(\boldsymbol{r}). \tag{20}$$

For a single, cylindrically symmetric defect at the origin, the simplest choice is

$$\theta(\boldsymbol{r}) = \kappa\varphi, \qquad \kappa \in \mathbb{Z}, \tag{21}$$

where φ is the azimuthal angle. The integer quantization follows from single-valuedness of the order parameter: under $\varphi \to \varphi + 2\pi$, the phase must change by $2\pi\kappa$ so that $e^{i\theta}$ returns to itself. With Eq. (21),

$$\boldsymbol{v}(r) = \frac{\hbar\kappa}{mr}\,\hat{\boldsymbol{\varphi}}. \tag{22}$$

The circulation around a loop C of radius r is quantized:

$$\oint_C \boldsymbol{v}\cdot d\boldsymbol{\ell} = \frac{\hbar\kappa}{m}\int_0^{2\pi} d\varphi = \frac{2\pi\hbar\kappa}{m}. \tag{23}$$

At this stage, *nothing* has been assumed about the density profile $n(\boldsymbol{r})$. The velocity field in Eq. (22) already implies that the phase configuration cannot be globally smooth: the field is irrotational for $r \neq 0$, yet it carries a nonzero circulation. This is the precise sense in which a vortex is a topological defect.

Why a vortex is "global" while a phonon is "local"

A phonon corresponds to smooth fluctuations of density and phase, with θ single-valued and $\oint \nabla\theta\cdot d\boldsymbol{\ell} = 0$ for loops far away. A vortex carries a nontrivial winding $\oint \nabla\theta\cdot d\boldsymbol{\ell} = 2\pi\kappa$, so it can be detected by a loop enclosing the defect even if the loop is arbitrarily far from the center.

Distributional vorticity from Stokes theorem.

The apparent paradox is that Eq. (22) suggests $\nabla\times\boldsymbol{v} = 0$ for $r \neq 0$, but Eq. (23) shows the circulation is nonzero. The reliable way to resolve this is to use Stokes theorem in the sense of distributions.

Consider a disk D of radius R centered at the origin. Stokes theorem gives

$$\int_D (\nabla\times\boldsymbol{v})\cdot\hat{\boldsymbol{z}}\, d^2r = \oint_{\partial D}\boldsymbol{v}\cdot d\boldsymbol{\ell} = \frac{2\pi\hbar\kappa}{m}. \tag{24}$$

Since the right-hand side is independent of R (as long as the disk encloses the defect), $(\nabla\times\boldsymbol{v})\cdot\hat{\boldsymbol{z}}$ must vanish pointwise for $r \neq 0$ but integrate to a nonzero constant. The unique distribution consistent with Eq. (24) is

$$\nabla\times\boldsymbol{v} = \frac{2\pi\hbar\kappa}{m}\,\delta^{(2)}(\boldsymbol{r})\,\hat{\boldsymbol{z}}. \tag{25}$$

Thus the vorticity is concentrated at the origin as a delta-function singularity: the phase field $\theta = \kappa\varphi$ is not globally regular, and the origin is the obstruction. From (25) one can also easily read out [1]

$$\mathbf{v}(\mathbf{r}) = \nabla\theta(\mathbf{r}) \sim \frac{\hat{z}\times\mathbf{r}}{r^2}. \tag{26}$$

[1] Actually (26) can also be directly derived from (21)

Why the density must vanish at the center and the emergence of a core profile.

Equation (25) indicates that the phase field is singular at the origin. In a condensate, this singularity cannot be realized with a nonzero amplitude everywhere, because the kinetic energy density contains a factor

$$|\nabla\psi|^2 = \left|\nabla\sqrt{n}\right|^2 + n(\boldsymbol{r})\,|\nabla\theta|^2, \qquad |\nabla\theta|^2 = \frac{\kappa^2}{r^2}. \tag{27}$$

We have used (26) for the estimation of $|\nabla\theta|^2$. If $n(\boldsymbol{r}) \to n_0 > 0$ as $r \to 0$, then the angular contribution $n|\nabla\theta|^2 \sim n_0\,\kappa^2/r^2$ would make the kinetic-energy integral diverge at the origin:

$$\int_0 dr\, r\, n_0 \frac{\kappa^2}{r^2} \sim \int_0 \frac{dr}{r} = \infty. \tag{28}$$

Therefore, a finite-energy vortex *requires* that the density is depleted at the center so that $n(\boldsymbol{r}) \to 0$ as $r \to 0$. In other words, the topological winding forces the system to create a core where the amplitude collapses, and precisely there the phase ceases to be well-defined.

This motivates the standard parametrization

$$\psi(r,\varphi) = \sqrt{n_0}\, f(r)\, e^{i\kappa\varphi}, \qquad f(0) = 0, \;\; f(\infty) = 1, \tag{29}$$

where the real profile $f(r)$ is *not* assumed a priori; it is determined by minimizing the GP energy functional. The length scale over which f heals to 1 is set by the healing length ξ, so one often writes $f(r) = f(r/\xi)$. We will derive the Euler–Lagrange equation for f and show explicitly that the core size is indeed $O(\xi)$.

Topological defect and the necessity of a core.

Changing the winding number enclosed by a loop requires a discontinuity in the phase field along the deformation. In a condensate, the only physical way to achieve this is for the density to vanish somewhere on the loop during the process, so that the phase becomes undefined at that point. This is why vortices are accompanied by a core of depleted density: it is not an arbitrary dynamical detail, but the mechanism that makes the topology well-defined.

3 Vortex Energy, Vortex Entropy and the BKT Phase Transition

3.1 Energy functional, vortex core equation, and the role of ξ

We work in two dimensions and (for now) ignore trapping potentials. The grand-canonical GP energy functional can be written in a form that matches many textbook derivations,

$$\mathcal{E}[\psi] = \int d^2r \left[-\frac{\hbar^2}{2m}\,\psi^*(\nabla^2\psi) + \frac{U}{2}|\psi|^4 - \mu|\psi|^2 \right], \qquad \mu = Un_0. \tag{30}$$

Substituting the isotropic vortex ansatz

$$\psi(r,\varphi) = \sqrt{n_0}\, f(r/\xi)\, e^{i\kappa\varphi}, \qquad \kappa \in \mathbb{Z}, \tag{31}$$

one finds, using $\nabla^2 = \frac{1}{r}\frac{\partial}{\partial r}\left(r\frac{\partial}{\partial r}\right) + \frac{1}{r^2}\frac{\partial^2}{\partial\varphi^2}$,

$$-\psi^*(\nabla^2\psi) = n_0\left[-\frac{f}{r}\frac{d}{dr}\left(r\frac{df}{dr}\right) + \frac{\kappa^2 f^2}{r^2} \right], \qquad |\psi|^2 = n_0 f^2, \qquad |\psi|^4 = n_0^2 f^4. \tag{32}$$

Therefore the vortex energy becomes

$$\mathcal{E} = \int d^2r \left\{ \frac{\hbar^2 n_0}{2m}\left[-\frac{f}{r}\frac{d}{dr}\left(r\frac{df}{dr}\right) + \frac{\kappa^2 f^2}{r^2} \right] + \frac{U}{2}n_0^2 f^4 - \mu n_0 f^2 \right\}. \tag{33}$$

Why $-\psi^*\nabla^2\psi$ is equivalent to $|\nabla\psi|^2$ (integration by parts)

The kinetic-energy term is often written as $\frac{\hbar^2}{2m}\int d^2r\,|\nabla\psi|^2$. The equivalence with Eq. (30) follows from integration by parts:

$$\int d^2r\,|\nabla\psi|^2 = \int d^2r\,(\nabla\psi^*)\cdot(\nabla\psi) = -\int d^2r\,\psi^*(\nabla^2\psi) + \int_{\partial\Omega} d\boldsymbol{\ell}\cdot(\psi^*\nabla\psi). \tag{34}$$

For an infinite system one may take Ω to be a disk of radius R and then send $R\to\infty$. For a single vortex, $\psi\to\sqrt{n_0}e^{i\kappa\varphi}$ at large r, hence $|\nabla\psi|\sim\sqrt{n_0}|\kappa|/r$. The boundary contribution in Eq. (34) scales as $\int_{\partial\Omega} d\ell\,|\psi||\nabla\psi|\sim(2\pi R)\sqrt{n_0}\cdot\sqrt{n_0}|\kappa|/R = O(1)$, i.e., it is independent of R. Such a boundary term does not affect the Euler–Lagrange equation for the core profile $f(r/\xi)$, and for energy differences ΔE (vortex minus uniform state) it can be absorbed into an R-independent constant (part of the "core energy"). Therefore one may freely use either representation of the kinetic term when deriving the vortex profile equation.

Minimizing $\mathcal{E}$ with respect to f gives the Euler–Lagrange equation. It is natural to rescale distance by the healing length ξ, writing $\tilde{r}=r/\xi$. Using

$$\frac{\hbar^2}{2m\xi^2} = \mu = Un_0, \tag{35}$$

one obtains the dimensionless *core equation*

$$-\frac{1}{2\tilde{r}}\frac{d}{d\tilde{r}}\left(\tilde{r}\frac{df}{d\tilde{r}}\right) + \frac{\kappa^2}{\tilde{r}^2}f + f^3 = f, \tag{36}$$

with boundary conditions $f(0)=0$ and $f(\infty)=1$. The solution satisfies $f(\tilde{r})\approx 1$ for $\tilde{r}\gg 1$ and is strongly suppressed for $\tilde{r}\lesssim 1$. Hence the vortex core size is set by ξ.

Why the core appears at $r\sim\xi$.

From Eq. (22), $|v(r)| = \hbar|\kappa|/(mr)$. At $r\sim\xi$,

$$|v(\xi)|\sim\frac{\hbar}{m\xi} = \sqrt{\frac{2\mu}{m}}\sim c, \tag{37}$$

up to a factor of order one. When the local flow approaches the sound speed, the condensate *cannot* sustain a uniform density without paying a large kinetic energy cost, so the density depletes to form a core. The healing length ξ is precisely the scale where this crossover becomes unavoidable within GP theory.

3.2 Logarithmic energy and why other contributions are finite

We now focus on a single vortex with $\kappa=1$ in a disk of radius R. Let $\Delta E\equiv\mathcal{E}[\text{vortex}]-\mathcal{E}[\text{uniform}]$ be the energy cost relative to the uniform condensate. Substituting the vortex ansatz $\psi(r,\varphi)=\sqrt{n_s}\,f(r/\xi)e^{i\kappa\varphi}$ into the 2D GP functional and subtracting the uniform energy density, one can write the difference in the explicit radial form

$$\Delta E = 2\pi\int_0^R dr\,r\left[\frac{\hbar^2 n_s}{2m}\left(\left(\frac{df}{dr}\right)^2+\frac{\kappa^2 f^2}{r^2}\right)+\frac{U}{2}n_s^2\,(f^2-1)^2\right]. \tag{38}$$

The key observation is that, for $r\gg\xi$, one has $f(r/\xi)\to 1$. Therefore, $\left(\frac{df}{dr}\right)^2$ and $(f^2-1)^2$ decay sufficiently fast at large r and do not generate any system-size dependence, whereas $\frac{\kappa^2 f^2}{r^2}\to\frac{\kappa^2}{r^2}$

produces a logarithm. In other words, the *only* term in Eq. (38) that can generate the $\ln(R/\xi)$ behavior is the far-field circulation energy coming from $\kappa^2 f^2/r^2$.

A simple estimate uses a step-function profile

$$f(r) \approx \begin{cases} 0, & r < \xi, \\ 1, & r > \xi. \end{cases} \tag{39}$$

Then the dominant system-size dependent contribution to ΔE is

$$\Delta E_{\log} \approx 2\pi \int_{\xi}^{R} dr\, r\, \frac{\hbar^2 n_s}{2m} \frac{\kappa^2}{r^2} = \frac{\hbar^2 n_s}{2m} 2\pi\kappa^2 \int_{\xi}^{R} \frac{dr}{r} = \frac{\pi\hbar^2 n_s}{m} \kappa^2 \ln\!\left(\frac{R}{\xi}\right). \tag{40}$$

For a single vortex $\kappa = 1$, this reduces to $\Delta E_{\log} = \frac{\pi\hbar^2 n_s}{m} \ln(R/\xi)$. The step-function approximation is not meant to describe the detailed core profile; rather, it isolates the universal long-distance tail $\sim 1/r$ in the velocity field and hence the universal $\ln(R/\xi)$ scaling.

Corrections due to a more accurate core profile change the energy by an $O(1)$ amount (independent of R) and are often referred to collectively as the "core energy".

Why the other terms are finite

To make the statement above controlled, we start from the differential equation obeyed by f. Writing $\tilde{r} \equiv r/\xi$ and using $\hbar^2/(2m\xi^2) = \mu = Un_s$, energy minimization yields

$$-\frac{1}{2\tilde{r}} \frac{d}{d\tilde{r}} \left(\tilde{r} \frac{df}{d\tilde{r}} \right) + \frac{\kappa^2}{\tilde{r}^2} f + f^3 = f, \qquad f(0) = 0, \;\; f(\infty) = 1. \tag{41}$$

■ **Region $r \gg \xi$: asymptotics and term-by-term convergence**
Before checking convergence term by term, we first extract the large-r asymptotics of the vortex profile f. The dimensionless profile $f(\tilde{r})$ ($\tilde{r} \equiv r/\xi$) satisfies

$$-\frac{1}{2\tilde{r}} \frac{d}{d\tilde{r}} \left(\tilde{r} \frac{df}{d\tilde{r}} \right) + \frac{\kappa^2}{\tilde{r}^2} f + f^3 = f, \qquad f(\infty) = 1. \tag{42}$$

For $\tilde{r} \gg 1$, write $f(\tilde{r}) = 1 - \eta(\tilde{r})$ with $0 < \eta \ll 1$. Linearizing Eq. (42) to first order in η yields

$$\eta'' + \frac{1}{\tilde{r}} \eta' - 4\eta - \frac{2\kappa^2}{\tilde{r}^2} \eta + \frac{2\kappa^2}{\tilde{r}^2} = 0. \tag{43}$$

In the far field, the last term provides an explicit source $\propto \tilde{r}^{-2}$. For any algebraically decaying $\eta \sim \tilde{r}^{-p}$, the derivative combination satisfies $\eta'' + \tilde{r}^{-1}\eta' \sim \tilde{r}^{-p-2}$, i.e., it is down by two additional powers of $\tilde{r}$ compared with η. Moreover, the term $-\frac{2\kappa^2}{\tilde{r}^2}\eta$ is also down by two extra powers relative to -4η. Therefore, to leading order in $1/\tilde{r}$, the only possible balance at order $\tilde{r}^{-2}$ is between -4η and the source term:

$$-4\eta + \frac{2\kappa^2}{\tilde{r}^2} \approx 0 \qquad \Longrightarrow \qquad \eta(\tilde{r}) \sim \frac{\kappa^2}{2} \frac{1}{\tilde{r}^2}. \tag{44}$$

Equivalently,

$$1 - f(r/\xi) \sim \frac{\kappa^2}{2} \frac{\xi^2}{r^2}, \qquad \frac{df}{dr} \sim O\!\left(\frac{\xi^2}{r^3}\right), \qquad f^2 - 1 \sim -\kappa^2 \frac{\xi^2}{r^2}, \qquad (f^2-1)^2 \sim \kappa^4 \frac{\xi^4}{r^4}. \tag{45}$$

Now we check each contribution in Eq. (38) for $r \in [\xi, R]$.
First, the circulation term approaches κ^2/r^2 and produces

$$2\pi \int_{\xi}^{R} dr\, r\, \frac{\hbar^2 n_s}{2m} \frac{\kappa^2 f^2}{r^2} = \frac{\pi\hbar^2 n_s}{m} \kappa^2 \ln\!\left(\frac{R}{\xi}\right) + O(1), \tag{46}$$

which is the only source of the $\ln(R/\xi)$ behavior.
Second, the radial-gradient term is convergent:

$$2\pi \int_\xi^R dr\, r\, \frac{\hbar^2 n_s}{2m} \left(\frac{df}{dr}\right)^2 \sim \int_\xi^R dr\, r\, \frac{1}{r^6} \sim \int_\xi^R \frac{dr}{r^5} = O(1), \tag{47}$$

independent of R as $R \to \infty$.
Third, the interaction/chemical-potential part is also convergent. Using $\mu = Un_s$,

$$\frac{U}{2} n_s^2 (f^2-1)^2 \sim \frac{U}{2} n_s^2 \frac{\xi^4}{r^4}, \qquad 2\pi \int_\xi^R dr\, r\, \frac{U}{2} n_s^2 (f^2-1)^2 \sim \int_\xi^R dr\, \frac{1}{r^3} = O(1). \tag{48}$$

Thus, for $r \gg \xi$, only the circulation term can accumulate a logarithm with system size.
■ **Region $r \lesssim \xi$: regularity at the origin and finiteness of the core contribution**
Near the origin, regularity and single-valuedness imply that f must vanish as a power,

$$f(\tilde{r}) \sim C\, \tilde{r}^{|\kappa|} \qquad (\tilde{r} \to 0), \tag{49}$$

which is consistent with the dominant balance in Eq. (42) between the radial derivatives and the $\kappa^2 f/\tilde{r}^2$ term.
With Eq. (49), the potentially dangerous factor $1/r^2$ is cancelled by f^2:

$$\frac{\kappa^2 f^2}{r^2} \sim \frac{\kappa^2 C^2}{\xi^{2|\kappa|}}\, r^{2|\kappa|-2}, \qquad \left(\frac{df}{dr}\right)^2 \sim \frac{C^2|\kappa|^2}{\xi^{2|\kappa|}}\, r^{2|\kappa|-2}. \tag{50}$$

Multiplying by the measure $2\pi r\, dr$, both contributions scale as $\int_0^\xi dr\, r^{2|\kappa|-1}$, which is finite for all integers $|\kappa| \geq 1$; in particular for a single vortex $|\kappa| = 1$ the integrand is $\sim r^1$ and is manifestly integrable at $r = 0$.
Finally, the interaction term $(f^2-1)^2$ is bounded in the core region, and the core occupies a finite area $\sim \pi\xi^2$, so its total contribution is also finite. Altogether, the entire $r \lesssim \xi$ region contributes only an $O(1)$ "core energy" and cannot generate any R-dependence.

3.3 Berezinskii–Kosterlitz–Thouless (BKT) transition from energy–entropy competition

At finite temperature, one must consider the free energy $\mathcal{F} = E - TS$. A single *free* vortex in a disk of radius R can be placed at $\sim R^2/\xi^2$ distinct positions, giving the entropy estimate

$$S \approx k_B \ln\left(\frac{R^2}{\xi^2}\right) = 2k_B \ln\left(\frac{R}{\xi}\right). \tag{51}$$

Combining Eqs. (40) and (51) yields the leading-size free energy of a single free vortex:

$$\mathcal{F} \approx \left(\frac{\pi\hbar^2 n_s}{m} - 2k_B T\right) \ln\left(\frac{R}{\xi}\right). \tag{52}$$

It is often useful to express the criterion in terms of the *thermal de Broglie wavelength*

$$\lambda = \sqrt{\frac{2\pi\hbar^2}{m k_B T}}, \tag{53}$$

so that Eq. (52) becomes

$$\mathcal{F} \approx \frac{k_B T}{2}\left(n_s \lambda^2 - 4\right) \ln\left(\frac{R}{\xi}\right). \tag{54}$$

The BKT theory interprets this as follows.

◦ When $n_s\lambda^2 > 4$, $\mathcal{F}$ grows with system size and free vortices are strongly suppressed; thermal fluctuations are dominated by tightly bound vortex–antivortex pairs.

◦ When $n_s\lambda^2 < 4$, $\mathcal{F}$ becomes negative in the thermodynamic limit and free vortices proliferate, destroying phase coherence and leading to an exponential decay of correlations.

Universal jump and "topological" nature of the transition

The BKT transition features a universal jump in the superfluid stiffness: in the simplest form, the criterion $n_s\lambda^2 = 4$ marks the point where the system ceases to sustain bound vortex–antivortex pairs as the dominant topological excitations. The transition is "topological" in the sense that it is driven by the (de)confinement of topological defects classified by $\Pi_1(U(1)) = \mathbb{Z}$, rather than by a conventional symmetry-breaking order parameter.

Relation to the XY model.

At long wavelengths, a 2D superfluid is described by an effective phase-only free energy $F_{\text{eff}} \approx \frac{\rho_s}{2}\int d^2r\,(\nabla\theta)^2$, which is precisely the continuum limit of the 2D XY model. The microscopic differences (e.g. the presence of amplitude fluctuations and a dynamically generated core size ξ in a BEC) affect short-distance details such as the core energy, but not the universal mechanism by which vortices drive the BKT transition.

4 Rotation: Effective Magnetic Field, Lowest Landau Level, and Vortex Lattices

4.1 Vortex entry and the critical rotation frequency

Consider a condensate in a trap rotating about the z-axis with angular frequency Ω. In the rotating frame, the energy functional acquires the term $-\Omega L_z$, where

$$\hat{L}_z = -i\hbar\frac{\partial}{\partial\varphi}. \tag{55}$$

For a vortex state with phase $e^{i\kappa\varphi}$, one has

$$\langle\hat{L}_z\rangle = \int d^2r\,\psi^*\left(-i\hbar\frac{\partial}{\partial\varphi}\right)\psi = \hbar\kappa\int d^2r\,|\psi|^2 = \hbar\kappa N, \tag{56}$$

where N is the particle number. Thus the rotational energy gain is approximately $-\Omega\hbar\kappa N$.

Balancing the vortex energy cost Eq. (40) with the rotational energy gain gives a crude estimate for the critical Ω_c where a vortex becomes energetically favorable. Using $N \approx n_s\pi R^2$ for a disk of radius R and taking $\kappa = 1$,

$$\frac{\pi\hbar^2 n_s}{m}\ln\!\left(\frac{R}{\xi}\right) - \Omega_c\,\hbar\,n_s\pi R^2 \approx 0, \tag{57}$$

which yields

$$\Omega_c \sim \frac{\hbar}{mR^2}\ln\!\left(\frac{R}{\xi}\right). \tag{58}$$

As Ω increases beyond Ω_c, more vortices enter the condensate. The next question is how these vortices arrange themselves in the energetically preferred configuration. Will they possibly form a lattice structure?

4.2 Single-particle Hamiltonian in the rotating frame and the effective magnetic field

A standard starting point is the single-particle Hamiltonian for a 2D harmonic trap of frequency ω rotating at Ω:

$$\hat{H}_0 = \frac{\hat{\boldsymbol{p}}^2}{2m} + \frac{1}{2}m\omega^2 r^2 - \Omega \hat{L}_z. \tag{59}$$

The key algebraic step is to complete the square. Using $\hat{L}_z = \hat{z} \cdot (\hat{\boldsymbol{r}} \times \hat{\boldsymbol{p}})$ and defining the vector potential

$$\boldsymbol{A}(\boldsymbol{r}) = m\Omega\, \hat{\boldsymbol{z}} \times \boldsymbol{r}, \qquad A_x = -m\Omega y, \quad A_y = m\Omega x, \tag{60}$$

one checks the identity

$$\frac{\hat{\boldsymbol{p}}^2}{2m} - \Omega \hat{L}_z = \frac{1}{2m}\Big(\hat{\boldsymbol{p}} - \boldsymbol{A}(\hat{\boldsymbol{r}})\Big)^2 - \frac{1}{2}m\Omega^2 r^2. \tag{61}$$

Substituting into Eq. (59) gives

$$\hat{H}_0 = \frac{1}{2m}\Big(\hat{\boldsymbol{p}} - \boldsymbol{A}(\hat{\boldsymbol{r}})\Big)^2 + \frac{1}{2}m(\omega^2 - \Omega^2)r^2. \tag{62}$$

This is formally identical to a charged particle in a magnetic field plus a residual trapping potential. The effective magnetic field is

$$\boldsymbol{B}_{\text{eff}} = \nabla \times \boldsymbol{A} = 2m\Omega\, \hat{\boldsymbol{z}}. \tag{63}$$

As $\Omega \to \omega$, the residual trap term becomes small and the dynamics approaches the Landau-level problem.

4.3 Lowest Landau level (LLL) structure and the origin of vortex lattices

In the fast-rotation limit $\Omega \to \omega$, the single-particle spectrum organizes into nearly degenerate Landau levels. The lowest Landau level (LLL) admits wavefunctions of the form

$$\psi(\boldsymbol{r}) = f(z)\, e^{-|z|^2/(2a^2)}, \qquad z = x + iy, \qquad a = \sqrt{\frac{\hbar}{m\Omega}}, \tag{64}$$

where $f(z)$ is an analytic function. Zeros of $f(z)$ correspond to points where ψ vanishes; near a zero, the phase winds and the point behaves as a vortex core. Thus, in the LLL regime, the positions of vortices are encoded directly as the zeros of an analytic function.

If vortices form a periodic lattice, one needs an analytic function whose zeros form a 2D Bravais lattice and whose quasi-periodicity is compatible with the effective magnetic translation symmetry. *Jacobi theta functions* provide precisely such analytic functions; they can be used as variational building blocks to construct LLL states with a prescribed vortex lattice.

Finally, in the LLL approximation, the single-particle energy is (nearly) degenerate, and the lattice geometry is selected by minimizing the interaction energy. For a contact interaction,

$$\mathcal{E}_{\text{int}} = \frac{U}{2}\int d^2 r\, |\psi(\boldsymbol{r})|^4. \tag{65}$$

This variational problem yields that the triangular (Abrikosov) lattice minimizes $\mathcal{E}_{\text{int}}$, explaining why vortex lattices in rapidly rotating single-component BECs are generically triangular.

A Topology and homotopy groups: what is being classified?

Topology studies *global* properties of spaces and maps that remain invariant under *continuous deformations*. In condensed-matter and many-body physics, topology typically enters through the following structural question: given an order parameter (or a set of low-energy fields) taking values in some manifold $\mathcal{M}$, which spatial configurations are *topologically distinct*, in the sense that they cannot be smoothly deformed into each other without leaving the space of physically admissible configurations?

A.1 From field configurations to maps $S^n \to \mathcal{M}$

A large class of topological classifications in physics can be phrased in terms of maps from a sphere S^n in real space into a target space $\mathcal{M}$ of internal degrees of freedom. The sphere S^n usually arises as the boundary of a region after excluding a defect core. Concretely, suppose a field $\Phi(\boldsymbol{r})$ is well-defined and constrained to lie in $\mathcal{M}$ outside some localized singular region (the "core"). Take a region Ω that encloses the core, and restrict Φ to the boundary $\partial\Omega$. If $\partial\Omega \simeq S^n$, then the configuration determines a continuous map

$$\Phi|_{\partial\Omega} : \; S^n \longrightarrow \mathcal{M}. \tag{66}$$

Different defect types correspond to different *homotopy classes* of such maps.

Two continuous maps $f, g : S^n \to \mathcal{M}$ are said to be *homotopic* if there exists a continuous interpolation

$$H : \; S^n \times [0,1] \longrightarrow \mathcal{M}, \qquad H(\cdot, 0) = f, \;\; H(\cdot, 1) = g. \tag{67}$$

Intuitively, H is a continuous deformation that turns one configuration into the other without ever becoming ill-defined on $\partial\Omega$. Homotopy is an equivalence relation, and the set of equivalence classes $[f]$ forms the n-th homotopy group, denoted

$$\Pi_n(\mathcal{M}). \tag{68}$$

Why a *group*?–composition by gluing)

The "group" structure comes from composing maps by gluing spheres along an equator (or, equivalently, by concatenating loops when $n = 1$). For $n = 1$, a map is a loop in $\mathcal{M}$ based at a reference point, and the group operation is simply traversing one loop followed by another. The identity is the contractible (constant) loop, and the inverse corresponds to reversing the direction.

A.2 Which homotopy group classifies which defect?

In d spatial dimensions, a defect of codimension q (i.e., of dimension $d - q$) is typically detected by surrounding it with a small sphere S^{q-1}. Thus the relevant classification is

$$\text{codimension } q \text{ defects in } d\text{-Dim} \quad \Longleftrightarrow \quad \Pi_{q-1}(\mathcal{M}). \tag{69}$$

This rule covers common examples:

- **Point defects in 2D** ($q = 2$): classified by $\Pi_1(\mathcal{M})$ (vortices in 2D superfluids, disclinations in 2D crystals, etc.).
- **Line defects in 3D** ($q = 2$): also classified by $\Pi_1(\mathcal{M})$ (vortex lines in 3D superfluids/superconductors).
- **Point defects in 3D** ($q = 3$): classified by $\Pi_2(\mathcal{M})$ (monopole/hedgehog defects in certain spin textures).

A.3 The BEC case: $\Pi_1(U(1)) = \mathbb{Z}$ and winding number

For a single-component Bose–Einstein condensate, the order parameter is a complex scalar $\psi = \sqrt{n}\, e^{i\theta}$. Whenever the density $n(\boldsymbol{r}) \neq 0$, the phase $\theta(\boldsymbol{r})$ is well-defined modulo 2π. Therefore the order-parameter manifold for the *phase degree of freedom* is

$$\mathcal{M} = U(1) \simeq S^1. \tag{70}$$

In a two-dimensional system, a point defect (vortex) is surrounded by a loop $\partial\Omega \simeq S^1$. Hence vortices are classified by maps $S^1 \to S^1$, i.e. by

$$\Pi_1(S^1) = \mathbb{Z}. \tag{71}$$

The integer invariant can be written as the winding number

$$\kappa = \frac{1}{2\pi} \oint_{\partial\Omega} \nabla\theta \cdot d\boldsymbol{\ell} \in \mathbb{Z}, \tag{72}$$

which counts how many times the condensate phase winds by 2π along a closed loop enclosing the defect. This is precisely the topological content behind circulation quantization in a superfluid: $\oint \boldsymbol{v} \cdot d\boldsymbol{\ell} = (\hbar/m)\, 2\pi\kappa$.

A.4 Examples beyond BEC: how the same mathematics appears across physics

The homotopy viewpoint is pervasive because it only depends on symmetry breaking and the resulting manifold $\mathcal{M}$, not on microscopic details.

■ **2D XY model and BKT physics**

In the classical (or quantum) XY model, the local spin is constrained to lie in a plane and can be parameterized by an angle θ, so the manifold is again S^1. Therefore $\Pi_1(S^1) = \mathbb{Z}$ vortices exist just as in a 2D superfluid. The Berezinskii–Kosterlitz–Thouless transition is then the thermal unbinding transition of vortex–antivortex pairs; its existence relies on the availability of these stable topological defects and on the logarithmic energy scaling of an isolated vortex.

■ **Heisenberg model: why no BKT transition in the isotropic case**

For an isotropic Heisenberg spin in 2D, the order parameter is a unit vector on the Bloch sphere, $\mathcal{M} = S^2$. Since $\Pi_1(S^2)$ is trivial, loops can be contracted to a point and there are no stable vortex-like point defects. This topological obstruction is why the BKT mechanism (as "vortex unbinding") does not apply.

■ **3D point defects and $\Pi_2(\mathcal{M})$**

In 3D, surrounding a point defect uses S^2. When $\Pi_2(\mathcal{M}) \neq 0$, one can have monopole/hedgehog defects. A familiar example is $\Pi_2(S^2) = \mathbb{Z}$, relevant for certain spin textures (e.g. skyrmion/hedgehog-type configurations depending on context). Whether such defects drive a BKT-like transition depends not only on their existence but also on how their energy scales with system size.

■ **Hopf invariant and $\Pi_3(S^2)$**

Some 3D textures are classified by $\Pi_3(S^2) = \mathbb{Z}$, whose integer is the Hopf invariant. Physically, it counts a linking structure of preimages under the map. Such invariants arise in knot-like solitons and certain topological field configurations, emphasizing that homotopy can classify objects beyond simple vortices and monopoles.

A.5 What this classification does *and does not* say

Homotopy groups classify *topological sectors* of admissible configurations under smooth deformations. This immediately provides robust, model-independent statements:

- whether stable defects can exist at all (e.g. $\Pi_1(\mathcal{M}) \neq 0$ for vortices);

- what discrete invariants label them (e.g. integer winding κ);
- which processes can change the invariant (only those that pass through a singular configuration where the order parameter is ill-defined, such as a vortex core crossing a loop).

However, homotopy alone **does not** determine the *energetics* (core size, core energy, interactions, transition temperature). Those quantitative properties require the dynamical theory (here the GP functional and its excitations), which is why in the main text we combine the topological classification with explicit energy estimates.

B Landau Levels: Magnetic Length, Degeneracy, and Holomorphic LLL Structure

B.1 Landau gauge solution: magnetic length and degeneracy counting

Consider a charged particle (charge q, mass m) in a uniform magnetic field $\boldsymbol{B} = B\hat{\boldsymbol{z}}$ in 2D:

$$\hat{H} = \frac{1}{2m}\big(\hat{\boldsymbol{p}} - q\boldsymbol{A}(\hat{\boldsymbol{r}})\big)^2. \tag{73}$$

Choose the Landau gauge $\boldsymbol{A} = (0, Bx, 0)$. Then

$$\hat{H} = \frac{1}{2m}\left[\hat{p}_x^2 + (\hat{p}_y - qBx)^2\right]. \tag{74}$$

Since $\hat{H}$ is independent of y, one has $[\hat{H}, \hat{p}_y] = 0$, and eigenstates can be chosen as

$$\psi(x, y) = e^{ik_y y}\,\phi(x), \qquad \hat{p}_y\psi = \hbar k_y \psi, \tag{75}$$

where the wave function has been explicitly separated in x and y directions.[2].

Substituting $\hat{p}_y \to \hbar k_y$ into Eq. (74) yields an effective 1D Hamiltonian

$$\hat{H}(k_y) = \frac{\hat{p}_x^2}{2m} + \frac{1}{2}m\omega_c^2(x - x_0)^2, \qquad \omega_c = \frac{|q|B}{m}, \qquad x_0 = \frac{\hbar k_y}{qB}. \tag{76}$$

Thus the spectrum is a harmonic oscillator:

$$E_n = \hbar\omega_c\left(n + \frac{1}{2}\right), \qquad n = 0, 1, 2, \ldots \tag{77}$$

independent of k_y. The characteristic length scale of the oscillator[3] is

$$\ell_B = \sqrt{\frac{\hbar}{m\omega_c}} = \sqrt{\frac{\hbar}{|q|B}}, \tag{78}$$

called the *magnetic length*.

■ **Degeneracy per Landau level**

Consider a rectangle $0 \le x \le L_x$, $0 \le y \le L_y$ with periodic boundary conditions in y:

$$\psi(x, y + L_y) = \psi(x, y) \quad \Rightarrow \quad k_y = \frac{2\pi}{L_y}m, \;\; m \in \mathbb{Z}. \tag{79}$$

[2]Note that the eigenvector of $\hat{p}_y$ is $e^{ik_y y}$. You should feel ashamed if you've forgotten this.

[3]The typical width of ground state Gaussian wave packet.

The guiding center is $x_0 = \hbar k_y/(qB)$. Requiring that the state is localized within the sample implies $x_0 \in [0, L_x]$, hence $k_y \in [0, (qB/\hbar)L_x]$. The number of allowed k_y values is

$$N_{\text{deg}} \approx \frac{(qB/\hbar)L_x}{2\pi/L_y} = \frac{|q|B}{2\pi\hbar} L_x L_y = \frac{|q|BA}{h}, \qquad A = L_x L_y. \tag{80}$$

Equivalently, the degeneracy density is

$$\frac{N_{\text{deg}}}{A} = \frac{|q|B}{h} = \frac{1}{2\pi\ell_B^2}. \tag{81}$$

This counting is the bulk statement behind the intuition "one state per flux quantum".

"One state per flux quantum" and the flux quantum

For a charged particle of charge q in a uniform magnetic field B, the magnetic flux through an area A is

$$\Phi \equiv \int_A \boldsymbol{B} \cdot d\boldsymbol{S} = BA \qquad \text{(uniform } B\text{)}. \tag{82}$$

The **flux quantum** is defined as

$$\Phi_0 \equiv \frac{h}{|q|}. \tag{83}$$

The Landau-level degeneracy in area A can be written as

$$N_{\text{deg}} = \frac{|q|BA}{h} = \frac{\Phi}{\Phi_0}. \tag{84}$$

Thus each Landau level provides *one single-particle state per flux quantum* piercing the sample: increasing the total flux by Φ_0 increases the degeneracy by exactly one.

B.2 Symmetric gauge and the holomorphic structure of the LLL

To expose the analytic structure, it's more convenient to use the symmetric gauge

$$\boldsymbol{A} = \frac{B}{2}(-y, x, 0). \tag{85}$$

Define the kinetic momenta $\boldsymbol{\Pi} = \boldsymbol{p} - q\boldsymbol{A}$, which satisfy

$$[\Pi_x, \Pi_y] = i\hbar qB. \tag{86}$$

Introduce ladder operators

$$\hat{a} = \frac{\ell_B}{\sqrt{2}\hbar}\big(\Pi_x - i\Pi_y\big), \qquad \hat{a}^\dagger = \frac{\ell_B}{\sqrt{2}\hbar}\big(\Pi_x + i\Pi_y\big), \tag{87}$$

so that $[\hat{a}, \hat{a}^\dagger] = 1$ and

$$\hat{H} = \hbar\omega_c\left(\hat{a}^\dagger\hat{a} + \frac{1}{2}\right). \tag{88}$$

Therefore the LLL condition is $\hat{a}\psi = 0$.

Introduce complex coordinates $z = x + iy$, $\bar{z} = x - iy$, and derivatives

$$\partial_z = \frac{1}{2}(\partial_x - i\partial_y), \qquad \partial_{\bar{z}} = \frac{1}{2}(\partial_x + i\partial_y). \tag{89}$$

A direct computation shows that $\hat{a}\psi = 0$ is equivalent (up to a nonzero constant factor) to the first-order equation

$$\left(\partial_{\bar{z}} + \frac{z}{4\ell_B^2}\right)\psi(z,\bar{z}) = 0. \tag{90}$$

This equation can be solved by the ansatz $\psi = e^{-|z|^2/(4\ell_B^2)} f(z)$. Substituting into Eq. (90) yields $\partial_{\bar{z}} f(z) = 0$, i.e. f is analytic. Thus,

$$\psi(z,\bar{z}) = f(z)\, e^{-|z|^2/(4\ell_B^2)}, \qquad f \text{ holomorphic.} \tag{91}$$

Zeros of $f(z)$ as vortices.

If $f(z)$ has an m-th order zero at $z = z_0$, then locally $f(z) \sim (z - z_0)^m$. Writing $z - z_0 = re^{i\varphi}$, one has $\psi \sim r^m e^{im\varphi} \times$ (nonzero): the density vanishes at $r = 0$ and the phase winds by $2\pi m$. Hence zeros of $f(z)$ encode vortices and their winding numbers.

B.3 Jacobi theta functions and vortex lattices in the LLL

To describe a periodic vortex lattice, one seeks a holomorphic function $f(z)$ whose zeros form a 2D lattice $\Lambda = \{nb_1 + mb_2\}$ and whose quasi-periodicity matches magnetic translations on the torus (periodic boundary conditions compatible with a nonzero magnetic flux). Jacobi theta functions provide canonical holomorphic functions with controlled quasi-periodicity:

$$\vartheta_1(u|\tau) \text{ has } \vartheta_1(u+\pi|\tau) = -\vartheta_1(u|\tau), \qquad \vartheta_1(u+\pi\tau|\tau) = -e^{-2iu-i\pi\tau}\vartheta_1(u|\tau), \tag{92}$$

and zeros arranged periodically in the complex plane. By choosing $u = \pi z/b_1$ and $\tau = b_2/b_1$, one can arrange zeros at lattice sites. Multiplying by an appropriate Gaussian and (if needed) an extra holomorphic prefactor ensures compatibility with the chosen gauge and boundary conditions, leading to an LLL wavefunction representing a vortex lattice.

The lattice shape (square, triangular, etc.) is then determined by interaction-energy minimization within the LLL manifold. For contact interactions, this yields the triangular Abrikosov lattice as the energetically preferred configuration.